Volume 10, Issue 3, 2020, 5665 - 5669 ISSN 2069-5837
Biointerface Research in Applied Chemistry
www.BiointerfaceResearch.com
https://doi.org/10.33263/BRIAC103.665669
Original Research Article Open Access Journal
Received: 14.02.2020 / Revised: 20.03.2020 / Accepted: 21.03.2020 / Published on-line: 29.03.2020

Study of the magnetic properties of Zn doped Cobalt ferrite ($CoZn_xFe_{2-x}O_4$)

Amrita Khan [1,*], Golam Dastegir Al-Quaderi [2], Mahabub Alam Bhuiyan [1], Kazi Hanium Maria [2], Shamima Choudhury [2], K M Amjad Hossain [3], Dilip Kumar Saha [3], Shirin Akhter [3]

[1]Department of Physical Sciences, Independent University, Bangladesh
[2]Department of Physics, University of Dhaka, Dhaka-1000, Bangladesh
[3]Materials Science Division, Atomic Energy Centre, Dhaka-1000

*corresponding author e-mail address: ***amrita@iub.edu.bd***

ABSTRACT

Zinc substitution is proposed as an efficient way to improve the performance of the ferrite. In this work, Zinc doped cobalt ferrite with the generic formula $CoZn_xFe_{2-x}O_4$, with x = 0.0, 0.1, 0.3 and 0.4 were prepared by conventional ceramic technique, sintered at 1000° C for 4 hours in air. The effect of zinc concentration on the initial permeability, Curie temperature, saturation magnetization, magnetic moment, coercivity and magnetic susceptibility was investigated. Contrary to most of the work in this subject, here Co is maintained fixed and Fe is progressively varied along with Zn. Curie temperature is found to increase initially up to 459 ^{0}C for Zn content of x = 0.1 and then decreased to 148^{0}C for further increase of Zn content (x = 0.4). Effect of Zn on the frequency dependent initial permeability, loss factor and relative quality factor was studied. The maximum value of saturation magnetization (51.37emu/gm) was found for the sample x = 0.1 and then decreases with the increase of Zn content. Morphological and magnetic properties of the samples were studied using scanning electron microscope (SEM) and vibrating sample magnetometer (VSM) respectively. The Zn-doped cobalt-ferrite (x = 0.1) having a high strain derivative could be a potential material for stress sensor application.

Keywords: *Cobalt-ferrite; Zn-doping; ceramic technique; saturation magnetization; permeability; coercivity; sensor application*

1. INTRODUCTION

Ferrites are ferromagnetic cubic spinels having simultaneous magnetic and dielectric properties. Physical properties of ferrites depend on their method of synthesis, chemical compositions, additives, sintering temperature and time, heating rate, etc [1,2]. Because of remarkable electronic and magnetic properties, ferrites have extensive use in industry. Spinel ferrites are widely used in many electronic devices because of their high permeability and saturation magnetization in the radio frequency (RF) region, high electrical resistivity, low eddy current, mechanical hardness, chemical stability and reasonable cost. Besides this, spinel ferrites have application in ferrofluid technology [3], magnetocaloric refrigeration [4], medical diagnostics [5], magnetic resonance imaging enhancement [6], etc. The general formula for the ferrites is MFe_2O_4, where M is a divalent metal ion like Mg, Mn, Cu, Ni, Co, Zn, Cd, etc, and Fe is trivalent. In spinel ferrites, cations occupy the tetrahedral (A) and octahedral (B) sites, named so depending on the number of oxygen atoms around them. The spinel structure (AB_2O_4), is based on a face-centered cubic lattice of oxygen atoms. The magnetic properties depend on the relative strengths of various exchange interactions between the magnetic moments on tetrahedral (A) sites and octahedral (B) sites. Cobalt ferrite ($CoFe_2O_4$) is well known to have a large magneto-crystalline anisotropy, high coercivity (~5×10^3 Oe), moderate saturation magnetization (~5×10^2 emu/g), high chemical stability and high mechanical hardness [7]. Due to these properties Cobalt ferrite is known to have used as a recording media. Properties of ferrites can be tailored not only by choosing a suitable synthesis method but also by choosing a suitable dopant. Co-Zn ferrites are important in the microwave industry since $CoFe_2O_4$ has long range ferromagnetic ordering and $ZnFe_2O_4$ has antiferromagnetic ordering [8]. $CoFe_2O_4$ has an inverse spinel structure with Co^{2+} ions in octahedral sites and Fe^{3+} ions equally distributed between tetrahedral and octahedral sites whereas $ZnFe_2O_4$ has a normal spinel structure with Zn^{2+} ions in tetrahedral and Fe^{3+} in octahedral sites. Therefore, Zn-substitution in $CoFe_2O_4$ may cause some distorted spinel structures depending upon the concentration of Zn. Substitution of magnetic Co or Fe ions by non-magnetic Zn results in a frustrated magnetic structure [9]. As a result within the spinel structure spin canting occurs and variation in the magnetization with respect to change of Zn content of the ferrite samples is expected to occur. It is therefore important to investigate the effect of Zn substitution on the structural, morphological and magnetic properties of Co-ferrites. Effects of the substitution of Co by Zn in Co-ferrites using ceramic technique [10], chemical co-precipitation [11] and sol-gel methods have been studied by different researchers. However, effect of the substitution of Fe by Zn in Co-ferrites has only been recently studied by authors for samples prepared using auto-combustion technique [12]. The effect of Zn on dielectric and transport properties of cobalt ferrite has been reported by the authors [13]. The present work reports the initial permeability, Curie temperature, saturation magnetization of Zn-substituted Co-ferrites prepared by the conventional double sintering solid-state reaction method. The study of these properties will have implications in industrial applications.

2. MATERIALS AND METHODS

Solid state reaction method was used to prepare Zn doped Cobalt ferrite $CoZn_xFe_{2-x}O_4$ (x = 0.0, 0.1, 0.3, 0.4). Oxides of iron (Fe_2O_3), cobalt (CoO) and zinc (ZnO) in required stoichiometric proportions were weighed first and then thoroughly mixed using ceramic mortar and pestle for 4 hours. The purity of raw materials used in the present work was of analytical research grade as supplied by the manufacturer E. Merck of Germany. The resultant powder was then ball milled for 4 hours to produce fine powder of mixed constituents. To avoid iron contamination, mixing was done with stainless steel balls in a steel ball milling machine and a fluid such as distilled water or acetone or ethanol was used to prepare the mixture into a slurry. The slurry prepared was dried, palletized and then transferred to a porcelin crucible for pre-firing at temperature of 800˚C in a Nabertherm furnace. Solid state reaction leading to the formation of ferrites was achieved by counter diffusion. In order to produce chemically homogenous and magnetically better material, this pre-fired lump material was crushed. This oxide mixture was again milled thoroughly for 4 hours to obtain homogenous mixture. Pressing the powder into compact desired shapes of two types- tablet and toroid was done by the help of a hydraulic press with a pressure of 2 ton/cm^2. The samples were then sintered at 1000˚ C for 4 hours to further homogenize the materials by completing the reactions left unfinished in the pre-firing step and to densify the samples.

The Scanning electron micrographs (SEM) of the prepared samples were observed with the magnification of 10,000 which are consistent with the previously reported X-ray diffraction (XRD) patterns [13]. Temperature dependence of initial permeability of the samples was measured using a laboratory built furnace and Wayne Kerr 3255B impedance analyzer and a thermocouple based thermometer from which Curie temperature of each sample was determined. Along with this, the frequency dependent permeability of the samples was measured using the same impedance analyzer. Measurement of magnetization was carried out by using an EV9 MICROSENSE VIBRATING SAMPLE MAGNETOMETER. The experiments were done at the laboratory of Materials Science Division, Atomic Energy Centre, Dhaka.

3. RESULTS

The scanning electron micrographs (SEM) (with magnification 10,000) of $CoZn_xFe_{2-x}O_4$ ferrites sintered at 1000˚C are shown in Figure 1. From these SEM, it is observed that with the increase in Zn content up to x=0.3, the porosity of the prepared samples decreases but with a further addition of Zn content (x=0.4), porosity increases, which may be attributed due to the existence of slight amount of metal oxides.

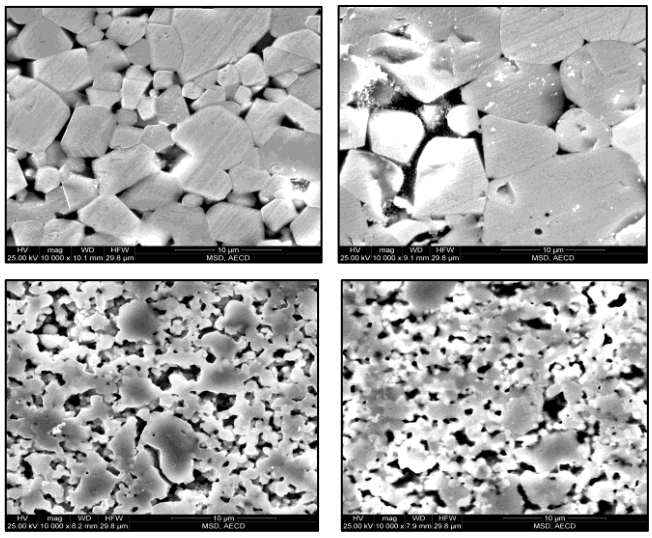

Figure 1. SEM of $CoZn_xFe_{2-x}O_4$ ferrite samples for x = 0.0, 0.1, 0.3 and 0.4.

Temperature dependent real part of initial permeability for prepared samples is shown in Figure 2. This temperature dependence of initial permeability can be explained on the basis of Globus model. According to this model, initial permeability μ_i' is given by,

$$\mu_i \propto \frac{M_S^2 D_m}{K_1} \qquad \textbf{(Eq. 1)}$$

Where, M_S is saturation magnetization, D_m is the average grain diameter and K_1 is the magneto-crystalline anisotropy constant. The anisotropy constant and saturation magnetization usually decreases with an increase in temperature due to thermal agitation which disturbs the alignment of the magnetic moments. However, anisotropy constant decreases much faster than saturation magnetization. When the anisotropy constant reaches zero, μ_i' attains its maximum value and then drop off to very low value. Thus the effect of K_1 is more significant in controlling the μ_i' of the ferrite materials. This behavior is the Hopkinson effect in permeability.

Variation of Curie temperature (T_c) with the variation of Zn content is shown in Figure 3. It is observed that the Curie temperature increases to 459^{0}C for x=0.1 and then decreases for the rest of the samples. This kind of behavior is also observed in some mixed ferrites with addition of non-magnetic Zn^{2+} ions [14]. This can be attributed to the fact that the Zn^{2+} ions of zero moment go to the A-sites, thus weakening the A-sites moment, and the Fe^{3+} ions have parallel moments in the B-sites, because of the strong A-B interaction. The expected net moment therefore increases. Thus the Curie temperature increases. Therefore, with additional Zn doping it is expected that the Curie temperature will increase. But this cannot occur because A moments will soon become too weak to affect the B moments and the net moment must sooner or later begin to decrease. As a result, a further decrease of Curie temperature is observed for the samples of x = 0.3, 0.4.

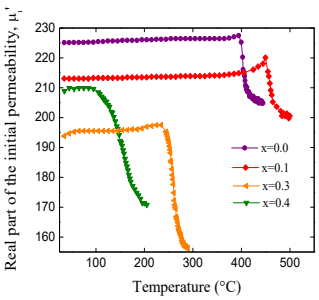

Figure 2. Temperature dependence of real part of initial permeability of $CoZn_xFe_{2-x}O_4$ (x = 0.0, 0.1, 0.3 and 0.4) sintered at 1000°C.

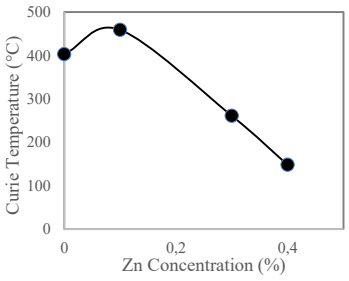

Figure 3. Variation of Curie Temperature as function of Zinc content for $CoZn_xFe_{2-x}O_4$.

The typical variation of real part (μ′) and imaginary part (μ′′) of initial permeability with frequency of the composition $CoZn_xFe_{2-x}O_4$ for x = 0.0, 0.1, 0.3 and 0.4 are shown in Figure 4 (a) and Figure 4 (b) respectively.

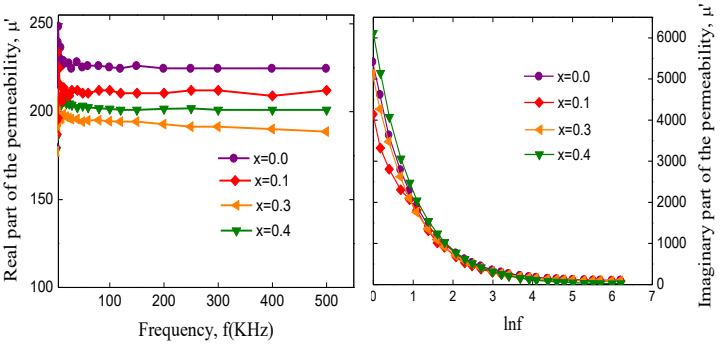

Figure 4. Real (left) and imaginary (right) parts of the permeability respectively as a function of frequency for the sample $CoZn_xFe_{2-x}O_4$ (x= 0.0, 0.1, 0.3 and 0.4).

From Figure 4 (a), it is evident that the value of real part of the permeability (μ′) is fairly constant over the frequency range which means that the sample prepared is compositionally stable and quality wise good. For high frequency application this property of μ′-f stability is an important criterion. Resonance is not observed because our facilities were restricted to measure up to 500 kHz frequency. But the samples resonance frequency is larger than that. So it was not possible to measure resonant frequency of the samples. Figure 4(b) represents the imaginary part of initial permeability, μ′′ (loss component) of the samples sintered at 1000°C. It is observed from the figure that μ′′ decreases with increasing frequency. The loss component decreases with increasing Zn content with x = 0.0-0.3 and increases for x = 0.4.

Effect of Zn content on the initial permeability (μ′) at a particular frequency of f = 100 kHz is shown in Table 1. From this table as well as Figure 4 (a), it is observed that the initial permeability decreases with Zn content for x = 0.0, 0.1 and 0.3 and increases for x = 0.4. The decrease may be due to the increase of anisotropy energy with the addition of non magnetic Zn^{2+} and the increase at x = 0.4 may be due to the sudden decrease in anisotropy constant for this composition [15].

From the permeability measurement, the loss factor tanδ or $D = \frac{\mu''}{\mu'}$ was calculated. Figure 5 shows the variation of loss factor with frequencies for different samples. The loss factor decreases with increasing frequency i.e., the magnetic loss is quite low for the samples showing it is a good candidate for a variety of applications like broadband pulse transformer [16].

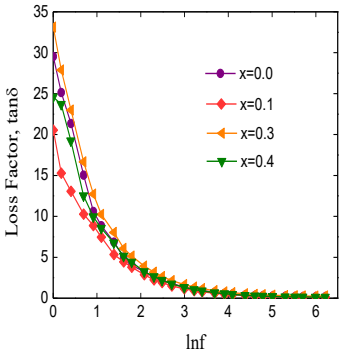

Figure 5. Loss factor (tanδ) vs. frequency (f) of the sample $CoZn_xFe_{2-x}O_4$.

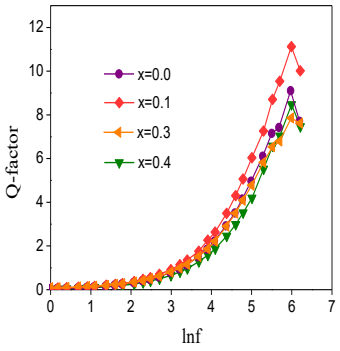

Figure 6. Relative Quality factor Vs frequency (f) of the sample $CoZn_xFe_{2-x}O_4$.

From the loss factor, the relative quality factor (Q-factor) was calculated. The Q-factor vs. frequency graph for all samples is shown in Figure 6. From Figure 6 it is observed that the value of Q-factor increases with the increase of frequency and shows a peak around 400 kHz for all the samples. The highest value of Q-factor is observed for the sample x = 0.1 and then Q_{max} decreases for rest of the samples. Q_{max} is found to decrease because of the increasing porosity [13]. The increasing amount of pore influences the loss factor to be increased which decreases the value of Q-factor. It is also observed that the loss factor is minimum and the quality factor is maximum for x = 0.1 i.e., $CoZn_{0.1}Fe_{1.9}O_4$ is a good candidate for high frequency applications.

The magnetic ordering in the simple spinel ferrites is based on the Neel's two sub lattices (tetrahedral A-site and octahedral B-site) model of ferrimagnetism in which the resultant magnetization is the difference between A-site and B-site magnetization, provided that they are co-linear and anti parallel to each other, i.e.,

$$M = M_B - M_A \qquad \textbf{(Eq. 2)}$$

Table 1. Real part of permeability of $CoZn_xFe_{2-x}O_4$ at frequency, f=100 kHz.

Zn content (x)	Real Part of Permeability μ_i' at 100 kHz
0.0	224.858
0.1	212.191
0.3	194.056
0.4	208.906

The magnetization depends on the distribution of Fe^{3+} ion between the tetrahedral (A) and octahedral (B) sites [1]. Pure $CoFe_2O_4$ has inverse spinel structure, whose cation distribution can be represented as,

$$(Co_x^{2+}Fe_{1-x}^{3+})[Co_{1-x}^{2+}Fe_{1+x}^{3+}]O_4 \qquad \textbf{(Eq. 3)}$$

where cations inside the round and square bracket occupy A and B site respectively. In our present sample Fe^{3+} has been substituted by Zn^{2+} ion. Zn^{2+} ion will replace the Fe^{3+} ion on the A-site.

Magnetic hysteresis loop and magnetization measured with the help of VSM (Vibrating Sample Magnetometer) for $CoZn_xFe_{2-x}O_4$ samples are shown in Figure 7 and 8, respectively.

From Figure 7 and Figure 8, it is observed that magnetization increases with Zn content up to x = 0.1 then decreases for further addition. The increase of magnetization is due to the dilution of magnetic moment of A sub-lattice by substitution of non-magnetic Zn ions. Since the resultant magnetization is the difference between the B and A sub-lattice magnetization as shown in equation 2, it is obvious that increase of net magnetization is expected on dilution of the A sub-lattice magnetization due to occupation of A-site by non-magnetic Zn content as well as enhancement of B sub-lattice magnetization due

to the introduction of Fe^{3+} ions having $5\mu_B$ migrated from A-site to B-site due to the occupation of Zn ion on the A-site.

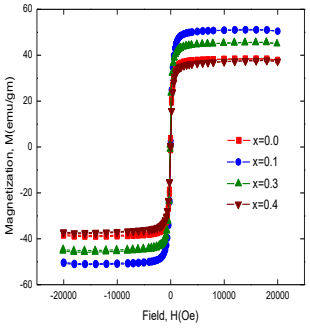

Figure 7. Magnetization curve measured at room temperature as a function of field of $CoZn_xFe_{2-x}O_4$ ferrites sintered at 1000°C for 4 hours.

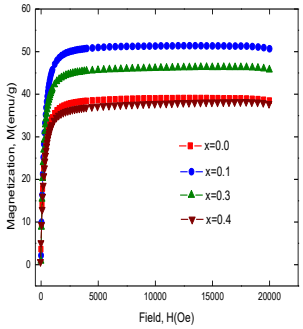

Figure 8. Saturation magnetization of different composition of $CoZn_xFe_{2-x}O_4$.

This rise of magnetization can be explained on the basis of Néel's two sub-lattice model. The decrease of magnetization after x = 0.1 at room temperature is due to the fact that the magnetization of A-sublattice is very dilute than that of B-sublattice. For this reason, the A-B exchange interaction becomes weaker comparable with the B-B exchange interactions. This disturbs the parallel alignment on the B-site paving way for canted spins of magnetic spin moments. Zn^{2+} and Cd^{2+} substituted ferrites have a potential to demonstrate a similar form of canting activity over a certain limit of their contents [17]. The presence of canted spin results in the Yafet-Kittel (Y-K) angle which compares the strength of A-B and B-B exchange interaction. Néel's two sublattice model is unable to explain the decrease of magnetization. The decrease of magnetization can be treated theoretically by triangular arrangement of spins as proposed by Yafet and Kittel [18]. Table 2 shows the values of Saturation magnetization, Coercivity and Remanence of $CoZn_xFe_{2-x}O_4$ (x = 0.0, 0.1, 0.3 and 0.4). The value of saturation magnetization for pure Cobalt ferrite is found to be 39.01 emu/gm which is much lesser than the reported value [12]. It could be due to the fact that we used Co_3O_4 as our raw material instead of CoO.

Table 2. Saturation magnetization, Coercivity and Remanence of $CoZn_xFe_{2-x}O_4$ (x = 0.0, 0.1, 0.3, 0.4).

Zn content, x	Saturation magnetization, M_S (emu/g)	Magnetic moment n_B (in μ_B)	Coercivity, H_C (Oe)	Remanence, M_R (emu/g)
0.0	39.011	1.56	22.577	2.2582
0.1	51.370	2.41	7.089	0.8204
0.3	46.064	1.86	7.155	0.8735
0.4	37.980	1.54	4.215	0.33

4. CONCLUSIONS

The magnetic properties and microstructure of Zn substituted cobalt ferrite ($CoZn_xFe_{2-x}O_4$, with x = 0.0, 0.1, 0.3 and 0.4) samples prepared by double sintering method were studied. The temperature dependent real part of initial permeability shows Hopkinson effect for all samples from which Curie temperatures were calculated. Curie temperature is found to increase initially with Zn content up to x=0.1 and then decrease for further increase of Zn content. This is due to the change of the iron distribution of A-site by non-magnetic Zn^{2+}. The initial permeability decreases with the increase in Zn content up to x=0.3 which is due to the increase of anisotropy energy with the addition of non magnetic Zn^{2+} but further increase in Zn content (x=0.4), it increases. This may be due to the sudden decrease in anisotropy constant for this composition. The highest value of Q-factor is observed for the sample x = 0.1 and then Q_{max} decreases for the rest of the samples. The increasing amount of pore influences the loss factor to be increased which decreases the value of Q-factor. The microstructures done by SEM showed that porosity decreases with Zn content up to x=0.3 but further addition of Zn content (x=0.4), porosity increases, which may be attributed due to the existence of slight amount of metal oxides. The increase in porosity refers to an increase in bond lengths in A and B sites which may decrease A-A and B-B interactions. The longer is the bond lengths, the higher is the porosity and lower is the magnetization, which could be useful for gas or humidity sensors. The saturation magnetization also increases up to x=0.1 and then decreases with an increase of x. These may be attributed to the variation of exchange interactions between the tetrahedral and octahedral sites. Thus Zn substitution plays an important role in the magnetic properties of cobalt ferrites.

5. REFERENCES

1. Goldman, A. *Modern Ferrite Technology.* 2nd ed.; Springer: New York, US, 2006; https://doi.org/10.1007/978-0-387-29413-1.
2. Jadhav, S.S.; Shirsath, S.E.; Toksha, B.G.; Shukla, S.J.; Jadhav, K.M. Effect of Cation Proportion on the Structural and Magnetic Properties of Ni-Zn Ferrites Nano-Size Particles Prepared By Co-Precipitation Technique. *Chinese Journal of Chemical Physics* **2008**, *21*, 381-386, https://doi.org/10.1088/1674-0068/21/04/381-386.
3. Acharya, P.; Desai, R.; Aswal, V.K. Upadhyay, R.V. Structure of Co-Zn ferrite ferrofluid: A small angle neutron scattering analysis. *Pramana – Journal of Physics* **2008**, *71*, 1069-1074, https://doi.org/10.1007/s12043-008-0225-7.
4. Mamiya, H.; Terada, N.; Furubayashi, T.; Suzuki H.S.; Kitazawa, H. Influence of random substitution on magnetocaloric effect in a spinel ferrite. *Journal of Magnetism and Magnetic Materials* **2010**, *322*, 1561-1564, https://doi.org/10.1016/j.jmmm.2009.09.023.
5. Kim, D.H.; Zeng, H.; Ng, T.C.; Brazel, C.S. T_1 and T_2 relaxivities of succimer-coated $MFe_2^{3+}O_4$ (M=Mn^{2+}, Fe^{2+} and Co^{2+}) inverse spinel ferrites for potential use as phase-contrast agents in medical MRI. *Journal of Magnetism and*

Magnetic Materials **2009**, *321*, 3899-3904, https://doi.org/10.1016/j.jmmm.2009.07.057.
6. Yang, H.; Zhang, C.; Shi, X.; Hu, H.; Du, X.; Fang, Y.; Ma, Y.; Wu, H.; Yang, S. Water-soluble superparamagnetic manganese ferrite nanoparticles for magnetic resonance imaging. *Biomaterials* **2010**, *31*, 3667-3673, https://doi.org/10.1016/j.biomaterials.2010.01.055.
7. Jadhav, S.S.; Shirsath, S.E.; Patange, S.M.; Jadhav, K.M. Effect of Zn substitution on magnetic properties of nanocrystalline cobalt ferrite. *Journal of Applied Physics* **2010**, *108*, https://doi.org/10.1063/1.3499346.
8. Pettit, G.A.; Forester, D.W. Mössbauer Study of Cobalt-Zinc Ferrites. *Physical Review B* **1971**, *4*, 3912. https://doi.org/10.1103/PhysRevB.4.3912.
9. Antoshina, L.G. The behaviour of the magnetostriction and magnetoresistance of the ferrite $CuGa_{0.4}Al_{0.8}Fe_{0.8}O_4$ with frustrated magnetic structure. *Journal of Physics: Condensed Matter* **2001**, *13*, 127, https://doi.org/10.1088/0953-8984/13/5/103.
10. Rana, M.U.; Ul-Islam, M.; Ahmed, I. Abbas, T. Determination of magnetic properties and Y–K angles in Cu–Zn–Fe–O system. *Journal of Magnetism and Magnetic Materials* **1998**, *187*, 242-246, https://doi.org/10.1016/S0304-8853(98)00077-8.
11. Han, Q.J.; Ji, D.H.; Tang, G.D.; Li, Z.Z.; Hou, X.; Qi, W.H.; Bian, R.R.; Liu, S.R. Dependence of magnetization on cation distributions in the spinel ferrites $Cu_{1-x}Zn_xFe_2O_4$ ($0.0 \le x \le 1.0$). *Physica Status Solidi A* **2012**, *209*, 766–772, https://doi.org/10.1002/pssa.201127646.
12. Somaiah, N.; Jayaraman, T.V.; Joy, P.A.; Das, D. Magnetic and magnetoelastic properties of Zn-doped cobalt-ferrites—$CoFe_{2-x}Zn_xO_4$ (x=0, 0.1, 0.2, and 0.3). *Journal of Magnetism and Magnetic Materials* **2012**, *324*, 2286–2291, https://doi.org/10.1016/j.jmmm.2012.02.116.
13. Khan, A.; Bhuiyan, M.A.; Al-Quaderi, G.D.; Maria, K.H.; Choudhury, S.; Hossain, M.A.; Akther, S.; Saha, D.K. Dielectric and transport properties of Zn-substituted cobalt ferrites. *Journal of Bangladesh Academy of Sciences* **2013**, *37*, 73-82, https://doi.org/10.3329/jbas.v37i1.15683.
14. Cullity, B.D.; Graham, C.D. *Introduction to Magnetic Materials*, 2nd ed.; John Wiley & Sons, Inc.: Hoboken, New Jersey, USA, 1972; https://doi.org/10.1002/9780470386323.
15. Bellad, S.S.; Watawe, S.C.; Shaikh, A.M.; Chougule, B.K. Cadmium substituted high permeability lithium ferrite. *Bulletin of Materials Science* **2000**, *23*, 83–85, https://doi.org/10.1007/BF02706546.
16. Kumar, P.; Sharma, S.K.; Knobel, M.; Singh, M. Effect of La^{3+} doping on the electric, dielectric and magnetic properties of cobalt ferrite processed by co-precipitation technique. *Journal of Alloys and Compounds* **2010**, *508*, 115-118, https://doi.org/10.1016/j.jallcom.2010.08.007.
17. Karche, B.R.; Khasbardar, B.V.; Vaingankar, A.S. X-ray, SEM and magnetic properties of Mg-Cd ferrites. *Journal of Magnetism and Magnetic Materials* **1997**, *168*, 292-298, https://doi.org/10.1016/S0304-8853(96)00705-6.
18. Yafet, Y.; Kittel, C. Antiferromagnetic Arrangements in Ferrites. *Physical Review* **1952**, *87*, 290, https://doi.org/10.1103/PhysRev.87.290.

6. ACKNOWLEDGEMENTS

The authors are grateful to the laboratory facilities of Materials Science Division, Atomic Energy Center, Dhaka, Bangladesh.